Engineering Science and Technology, an International Journal 18 (2015) 185–193

HOSTED BY

Contents lists available at ScienceDirect

Engineering Science and Technology, an International Journal

journal homepage: http://www.elsevier.com/locate/jestch

Full length article

Simulation of flow through dam foundation by isogeometric method

Mehrdad Shahrbanozadeh*, Gholam-Abbas Barani, Saeed Shojaee

Department of Civil Engineering, Shahid Bahonar University, P.O.BOX 76169133, Kerman, Iran

ARTICLE INFO

Article history:
Received 15 July 2014
Received in revised form
14 November 2014
Accepted 14 November 2014
Available online 2 January 2015

Keywords:
Seepage
Uplift force
Exit gradient
Isogeometric analysis
Experimental model

ABSTRACT

This research introduces a numerical approach called IsoGeometric Analysis (IGA) to solve the Laplace equation. Non-Uniform Rational B-Splines (NURBS) basis function is applied for approximation of the anisotropic saturated porous media of dam foundation field, as for description of the geometry. The discretized form of the governing Laplace equation is obtained using the standard Galerkin method. The present results consist of uplift pressure, seepage discharge and exit gradient which are validated with existing experimental data based on a physical model. The obtained data are also compared with empirical data. The computed results show a satisfactory agreement with the experimental measurements in the wide ranges of upstream flow conditions. In addition, it was found that the mentioned numerical method improves the convergency and accuracy of parameters compared to traditional methods.

1. Introduction

Dams usually are built on permeable foundations. Seepage through the dam foundation occurs due to the difference in water levels between the upstream and downstream sides and its effects on permeable foundations include the uplift force, seepage discharge and exit gradient. The uplift force reduces the shear resistance between the dam and its foundation. In addition, this process can provide strain, tension and finally decreasing safety factor against sliding or overturning of the dam structure. The exit gradient is the main design criterion in determining the safety of hydraulic structures against the piping phenomenon. Bligh (1910) introduced the creep length theory of the flow passing under hydraulic structures. He defined the creep length as the route of the first line of seepage which is in contact with the dam foundation. Also, Bligh stated that hydraulic gradient is constant along the creep line and energy loss along this path varies linearly with creep length. Thus, uplift pressure distribution is linear under the dam foundation [1,2].

Lane (1935) investigated the exit gradient for more than 200 damaged hydraulic structures and reported that there is a difference between horizontal and vertical creep paths. Consequently, he presented weighted creep theory in which coefficients of 0.33 and 1.0 for total horizontal and vertical percolation lengths were assigned, respectively (Fig. 1). Therefore, according to Lane's weighted creep theory, the equivalent creep length is defined in form of [2]:

$$L_{eq} = \frac{1}{3}\sum L_H + \sum L_V \tag{1}$$

in which L_{eq} is the total equivalent length, $\sum L_H$ is the total horizontal percolation length (walls with slope less than 45°) and $\sum L_V$ is the total vertical percolation length (walls with slope more than 45°). According to the Bligh's method, the uplift pressure distribution under the dam foundation is linear. To prevent undermining phenomenon at downstream toe of the structure, the available exit gradient (i_x) should be less than the allowable exit gradient (C) in following term:

$$i_x = \frac{\Delta h}{L_{eq}} \le C \rightarrow \frac{L_{eq}}{\Delta h} \ge \frac{1}{C} \Rightarrow L_{eq} \ge \frac{\Delta h}{C} \tag{2}$$

where Δh is difference between upstream and downstream heads:

Khosla et al. (1936) presented a method to estimate the distribution of uplift pressure under foundations through solving complex potential functions. They investigated the flow network under a hydraulic structure which was constructed on a permeable foundation. Khosla assumed that flow and potential lines are concentric ellipses and hyperbolic, respectively. Considering no

* Corresponding author.
E-mail addresses: m.Shahrbanozadeh@eng.uk.ac.ir (M. Shahrbanozadeh), gab@mail.uk.ac.ir (G.-A. Barani), Saeed.Shojaee@mail.uk.ac.ir (S. Shojaee).

Peer review under responsibility of Karabuk University.

http://dx.doi.org/10.1016/j.jestch.2014.11.001

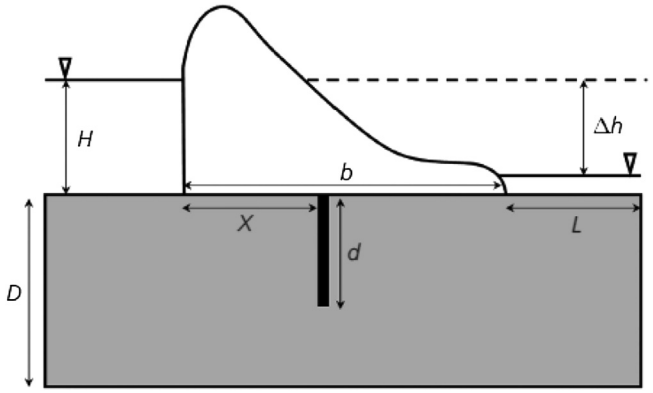

Fig. 1. A schematic definition for characterization of parameters in creep theory (Tokaldani and Shayan, 2012).

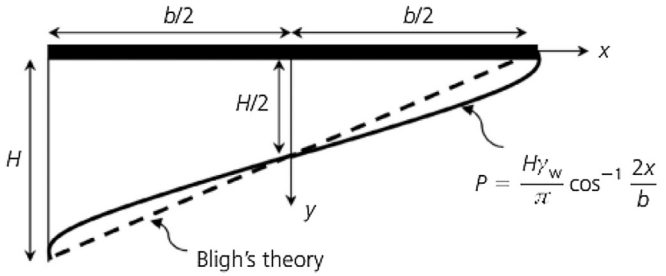

Fig. 2. Comparison of uplift distribution according to the Bligh and Khosla et al. Theories (Tokaldani and Shayan, 2012).

cutoff wall, the relationship of Khosla to estimate the uplift pressure distribution along the floor is [2,4].

$$P = \frac{H\,\gamma_w}{\pi}\cos^{-1}\frac{2x}{b} \quad \text{for } -\frac{b}{2} \le x \le \frac{b}{2} \tag{3}$$

and the exit gradient as:

$$i_{exit} = \frac{H}{\pi d\sqrt{Y}} \tag{4}$$

Here, H is upstream head and the parameters $Y = 1 + \sqrt{1+\alpha^2}/2$ and $\alpha = b/d$ varied by the length of foundation (b) and the length of cutoff wall(d) [2].

Fig. 2 illustrates the uplift distribution predicted by Bligh and Khosla theories. Although the theory of Khosla is generally more reliable than the creep theories of Bligh and Lane, in cases dealing with a compound foundation it is required to solve very complicated equations and also has a low accuracy when applied to anisotropic foundations [3].

The other methods for estimation of the uplift pressure under hydraulic structures are suggested based on solving the governing equations on problem condition. During the past century, various efforts were conducted to develop numerical modeling using the Darcy law and Richard equation. In a case study, Abedi Koupaei (1991) predicted the distribution of uplift pressure using the finite difference method [5].

In the recent decades, due to the high complexity of flow in porous media and in most cases, all domains of porous media were considered as a control system to be possible measuring the different hydraulic parameters between the particles. In this way, several investigators proposed the empirical relationships between hydraulic gradient and flux rate based on experimental data sets [6–10].

Also, due to the essential needs for investigations of 2D-(or 3D) dimensional problems and limitations of previous empirical models, applications of improved models have been studied by few researchers [11,12]. The IGA is a recently developed computational approach that offers the possibility of integrating finite element analysis (FEA) into conventional NURBS-based Computer Aided Design (CAD) tools. The IGA-based approaches have constantly developed and shown many great advantages on solving many different problems in a wide range of research areas such as fluid–structure interaction, shells, structural analysis and so on [14–18]. The concept of the IGA in mechanic problems is pioneered by Hughes and his co-workers as a novel technique for the discretization of partial differential equations [13]. Within recent years, the IGA has been applied to various flow problems and proved its value within the field of fluid mechanics. The first studies were in field of steady-state incompressible Stokes flow in the benchmarking lid-driven square cavity [14]. Subsequent analysis of the full time dependent Navier-Stokes equations using the IGA has shown its advantages for both variables continuity and complicated dynamic flow domains [15,16]. The basic idea of the IGA method is to utilize the basis functions that are able to model geometries exactly from the CAD points of view for numerical simulations of physical phenomena. It can be achieved using the B-splines or Non Uniform Rational B-splines (NURBS) for the geometrical description and invoke the isoparametric concepts to define the unknown field variables. The IGA-based approaches have constantly developed and shown several important advantages in solving different problems such as fluid-structure interaction, shells, and structural analysis [17–20]. Imposing essential boundary conditions in time dependent problems are applied in IGA with Hughes et al. [21].

In this paper, the numerical algorithm based on the IGA has been used to estimate the solution of the Laplace equation in anisotropic porous media. The results of the numerical model was compared with those obtained using the physical model based on experimental conditions and traditional methods.

2. Specifications of experimental model

In this study, data reported from experimental set up were applied to validate the proposed numerical model. The experiments were carried out in a flume with a length of 1.70 m and width of 0.18 m. The flume was located in the Hydraulic Laboratory of the Department of Irrigation and Reclamation Engineering, University of Tehran. To obtain hydraulic parameters and also the accuracy and the convergency of the proposed method, the experimental set consisted of an upstream impervious bed, an impervious wall as a dam body, various cutoff walls and a piezometric network. A schematic sketch of physical model was illustrated in Fig. 3. The length of cutoff walls varied from 2.5 cm to 30 cm and were located in different positions beginning from 40 cm upstream to 115 cm downstream from the impervious wall. The upstream head water was taken from 2.5 cm to 20 cm and the upstream water level was fixed by using a floating body. The downstream water level was set to zero. Distribution of uplift pressure was measured by the piezometric network, which consisted of 39 piezometers (13 rows with each row including 3 piezometers, Fig. 3) [3].

To prevent uncontrolled piping, a gravel filter ($D_{50} = 2$ mm) was dumped in both upstream and downstream beds. Beach sand, classified as the most unsuitable type of soil from the point of view of stability of hydraulic structures, was selected as pervious bed material. The hydraulic conductivity of the soil was measured using

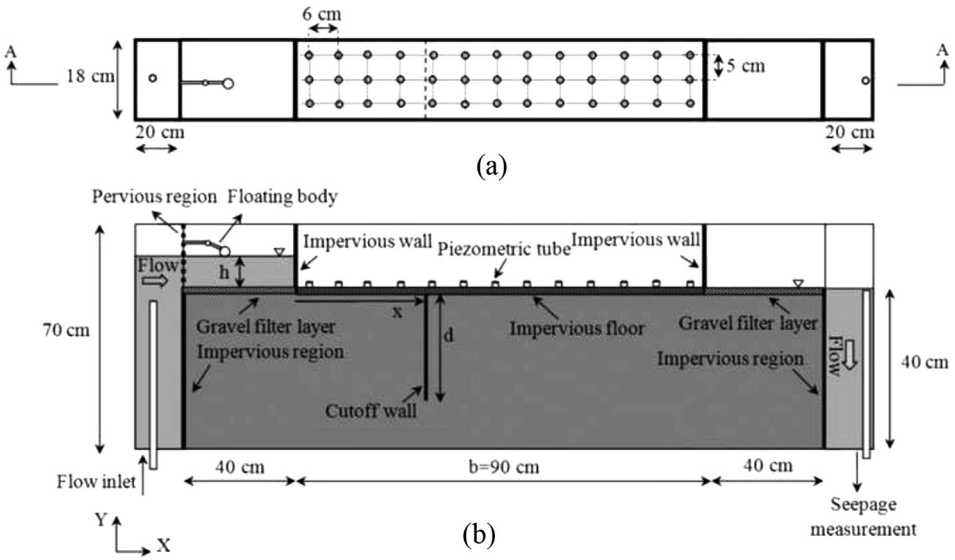

Fig. 3. Dimensions of the physical model: (a) Plan; (b). Section A-A. (Tokaldani and Shayan, 2012)

the constant-head method and injected dye. The soil horizontal and vertical hydraulic conductivities were estimated as 0.00143 m/s and 0.001202 m/s, respectively. A total of 110 experiments were conducted in various conditions of upstream heads, cutoff depths and cutoff wall positions. In each experiment, the seepage discharge was measured based on a volumetric method. Uplift pressure distribution was taken by reading water levels in piezometeric tubes [3].

3. The governing equation

Consider the time independent equation governing the flow in the two dimensional anisotropic region Ω with total boundary $\Gamma \equiv \partial\Omega$,

$$k_x\frac{\partial^2 u}{\partial x^2} + k_y\frac{\partial^2 u}{\partial y^2} = 0 \tag{5}$$

With boundary conditions as

$$\begin{cases} u = g \ \text{ on } \ \Gamma_D \\ k_x\dfrac{\partial u}{\partial x}n_x + k_y\dfrac{\partial u}{\partial y}n_y = h \ \text{ on } \ \Gamma_N \end{cases} \tag{6}$$

Where u is the total head at any point (x, y), Γ_D is the essential boundary condition, Γ_N is the natural boundary condition, g is the amount of u over essential boundary condition, h is the derivative of u over natural boundary condition, n_x and n_y are the components of the unit normal to the boundary, k_x and k_y are the horizontal and vertical hydraulic conductivity, respectively.

4. The isogeometric analysis

The concept of IGA is based on applying the NURBS basis functions in accurate modeling of geometry and approximation of solution space. The NURBS basis functions are weighted functions which originate from B-spline interpolation. The B-spline functions are defined on a knot vector. A knot vector is a suite of non-descending real numbers, which is presented by,

$$\Xi = \{\xi_1, \xi_2, \xi_3, \ldots, \xi_{n+p+1}\} \tag{7}$$

where ξ_i is the ith knot value, n and p are respectively the number and the order of basic functions defined in the knot vector. The first order B-spline is defined in the knot vector by,

$$N_{i,0}(\xi) = \begin{cases} 1 & \text{if} \quad \xi_i \le \xi < \xi_{i+1} \\ 0 & \text{otherwise} \end{cases} \tag{8}$$

and higher order basis functions are recursively defined by,

$$N_{i,p}(\xi) = \frac{\xi - \xi_i}{\xi_{i+p} - \xi_i}N_{i,p-1}(\xi) + \frac{\xi_{i+p+1} - \xi}{\xi_{i+p+1} - \xi_{i+1}}N_{i+1,p-1}(\xi) \tag{9}$$

In which $N_{i,p}$ is the ith basis function with p order. The NURBS basis functions are made from B-spline functions for two dimensional by equation in form of:

$$R^{p,q}_{i,j}(\xi,\eta) = \frac{N_{i,p}(\xi)\ M_{j,q}(\eta)\ \omega_{i,j}}{W(\xi)} \tag{10}$$

In which $\omega_{i,j}$ is the weight corresponding to i,j*th* control point. Also, W(ξ) is weight function that formulated by:

$$W(\xi) = \sum_{i=1}^{n}\sum_{j=1}^{m} N_{i,p}(\xi)M_{j,q}(\eta)\omega_{i,j} \tag{11}$$

The derivatives of B-spline basis functions are efficiently represented in terms of B-spline lower order basis. For a given polynomial order p and knot vector Ξ, the derivative of the ith basis function is given as follows:

$$\frac{d}{d\xi}N_{i,p}(\xi) = \frac{p}{\xi_{i+p} - \xi_i}N_{i,p-1}(\xi) - \frac{p}{\xi_{i+p+1} - \xi_{i+1}}N_{i+1,p-1}(\xi) \tag{12}$$

The higher derivatives was met by continual differentiating each side of Eq. (12) as

$$\frac{d^k}{d^k\xi}N_{i,p}(\xi) = \frac{p}{\xi_{i+p} - \xi_i}\left(\frac{d^{k-1}}{d^{k-1}\xi}N_{i,p-1}(\xi)\right) - \frac{p}{\xi_{i+p+1} - \xi_{i+1}}\left(\frac{d^{k-1}}{d^{k-1}\xi}N_{i+1,p-1}(\xi)\right) \tag{13}$$

Making use of control net $B_{i,j}$ i = 1, 2,…,n, *j* = 1, 2,…, m,

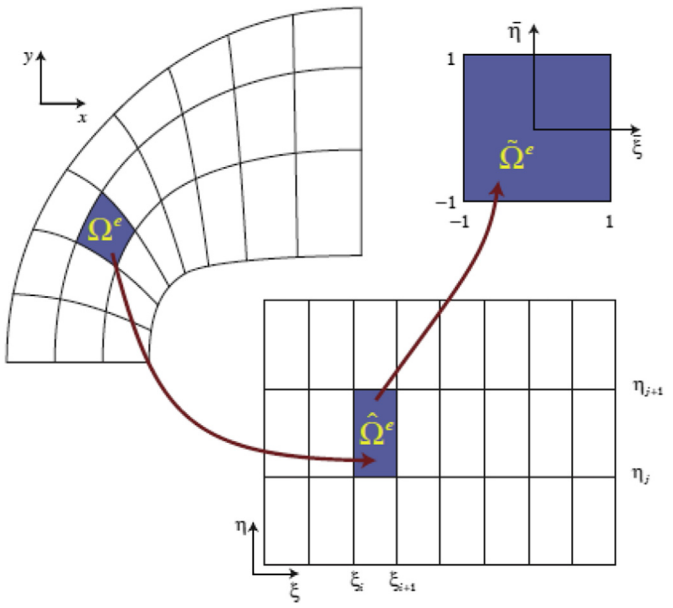

Fig. 4. Layout of space solution IGA(Hughes et al., 2005).

polynomial order p and q, and knot vectors $\Xi = \{\xi_1, \xi_2, \ldots, \xi_{n+p+1}\}$, and $H = \{\eta_1, \eta_2, \ldots, \eta_{m+q+1}\}$, a tensor product spline surface is defined as:

$$S(\xi, \eta) = \sum_{i=0}^{n} \sum_{j=0}^{m} N_{i,p}(\xi)\ M_{j,q}(\eta)\ B_{i,j} \tag{14}$$

Where $N_{i,\,p}(\xi)$ and $M_{j,q}(\eta)$ are univariate B-spline basis functions of order p and q, corresponding to knot vectors Ξ and H, respectively.

As seen in Fig. 4, we have denoted the element in the physical space by Ω^e and in the parameter space by $\widehat{\Omega}^e$, and so let us denote the parent element by $\tilde{\Omega}^e$. The integrals are pulled back, first onto the parametric domain and then onto a bi-unit parent element. The actual integration is performed by the Gaussian quadrature.

4.1. Discretization of governing equation

It was assumed that S and V are the subspaces of function space with continuous second derivative,

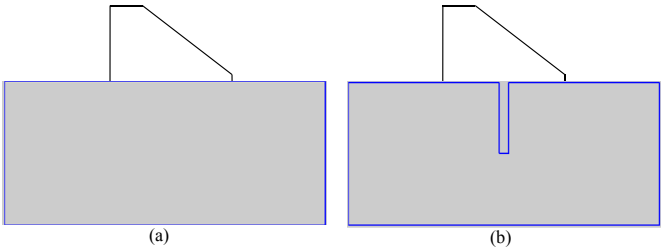

Fig. 5. (a) Domain of dam foundation without cutoff wall (b) with cutoff wall.

$$S = \left\{ f \middle| f \in H^1(\Omega), f\big|_{\Gamma_D} = g \right\} \tag{15a}$$

$$V = \left\{ r \middle| r \in H^1(\Omega), r\big|_{\Gamma_D} = 0 \right\} \tag{15b}$$

Where $H^1(\Omega)$ is Sobolev space and can be defined as follows:

$$H^1(\Omega) = \left\{ u | D^\alpha u\ \varepsilon\ L^2(\Omega), |\alpha| \le 1 \right\} \tag{16}$$

The Eq. (5) is a strong form of the boundary value problem that governs the state of the fluid. The semi discrete weak variational formulation of Eq. (5) over Ω can be expressed by multiplying Eq. (5) at an arbitrary test function w and applying Green-Gauss theory is given by

$$\int_\Gamma w\left(k_x \frac{\partial u}{\partial x} n_x + k_y \frac{\partial u}{\partial y} n_y\right) d\Gamma - \int_\Omega \nabla w \cdot \begin{bmatrix} k_x \frac{\partial u}{\partial x} \\ k_y \frac{\partial u}{\partial y} \end{bmatrix} d\Omega = 0 \tag{17}$$

or

$$\int_{\Gamma_D} w\left(k_x \frac{\partial u}{\partial x} n_x + k_y \frac{\partial u}{\partial y} n_y\right) d\Gamma - \int_{\Gamma_N} w\left(k_x \frac{\partial u}{\partial x} n_x + k_y \frac{\partial u}{\partial y} n_y\right) d\Gamma - \int_\Omega \nabla w \cdot \begin{bmatrix} k_x \frac{\partial u}{\partial x} \\ k_y \frac{\partial u}{\partial y} \end{bmatrix} d\Omega = 0 \tag{18}$$

Where

Table 1
Specifications of the geometric analysis.

a. Dam foundation without cutoff wall																						
Degree	p = q = 2																					
Knots	Ξ = {0,0,0,.5,.5,1,1,2,2,2}, H = {0,0,0,1,1,1}																					
Points	1	2	3	4	5	6	7	8	9	10	11	12	13	14	15	16	17	18	19	20	21	
x_i	0	0	0	2	.2	.2	.4	.4	.4	.85	.85	.85	1.3	1.3	1.3	1.5	1.5	1.5	1.7	1.7	1.7	
y_i	0	.2	.4	0	.2	.4	0	.2	.4	0	.2	.4	0	.2	.4	0	.2	.4	0	.2	.4	
ω	1	1	1	1	1	1	1	1	1	1	1	1	1	1	1	1	1	1	1	1	1	
b. Dam foundation with cutoff wall																						
Degree	p = q = 2																					
Knots	Ξ = {0,0,0,.5,.5,1,1,2,2,2}, H = {0,0,0,1,1,1}																					
Points	1	2	3	4	5	6	7	8	9	10	11	12	13	14	15	16	17	18	19	20	21	
x_i	.825	.4	0	.825	.4	0	.825	.4	0	.85	.85	.85	.875	1.3	1.7	.875	1.3	1.7	.875	1.3	1.7	
y_i	.4	.4	.4	.3	.24	.2	.825	.4	0	.85	.85	.85	.875	1.3	1.7	.875	1.3	1.7	.875	1.3	1.7	
ω	1	1	1	1	1	1	1	1	1	1	1	1	1	1	1	1	1	1	1	1	1	

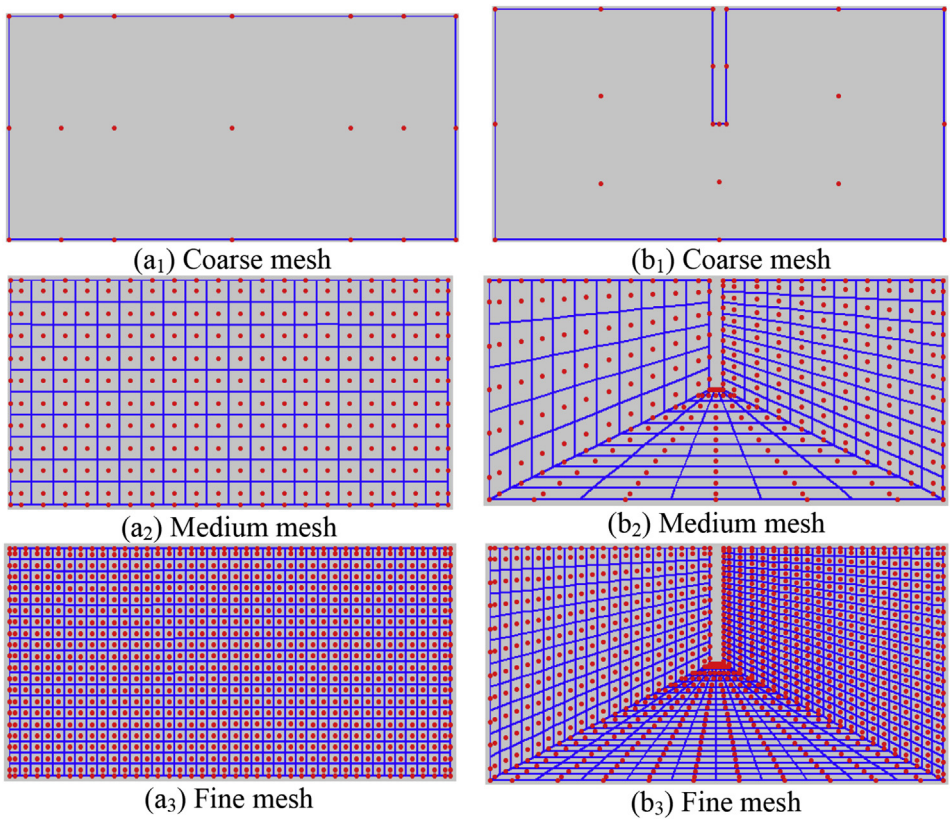

Fig. 6. Control mesh and physical mesh model of the dam foundation. (Left) no cutoff wall with cubic NURBS basis functions with 21, 264 and 924 control points and 6, 200 and 800 elements (Right) with cutoff wall with cubic NURBS basis functions with 21, 288 and 968 control points and 6, 200 and 800 elements. Blue lines mark the element boundaries and red circles are control points.

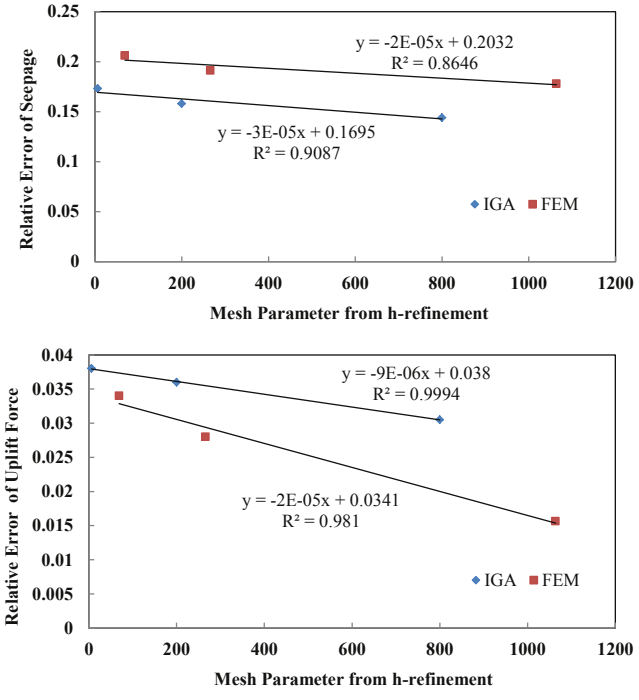

Fig. 7. Convergence of the relative error in the L^2-norm of seepage and uplift force for IGA and FEM discretizations.

$$\int_{\Gamma_D} w\left(k_x\frac{\partial u}{\partial x}n_x + k_y\frac{\partial u}{\partial y}n_y\right)d\Gamma = 0\ ,$$
$$\int_{\Gamma_N} w\left(k_x\frac{\partial u}{\partial x}n_x + k_y\frac{\partial u}{\partial y}n_y\right)d\Gamma = \int_{\Gamma_N} whd\Gamma \tag{19}$$

Using the essential boundary condition, u can be defined as,

$$u = v + g \in S,\ g \in V \tag{20}$$

Inserting this function into Eq. (18) yields:

$$\int_{\Gamma_N} whd\Gamma - \int_{\Omega} \nabla w \cdot \begin{bmatrix} k_x\frac{\partial v}{\partial x} \\ k_y\frac{\partial v}{\partial y} \end{bmatrix} d\Omega - \int_{\Omega} \nabla w \cdot \begin{bmatrix} k_x\frac{\partial g}{\partial x} \\ k_y\frac{\partial g}{\partial y} \end{bmatrix} d\Omega = 0 \tag{21}$$

or

$$\int_{\Gamma_N} whd\Gamma - \int_{\Omega} \nabla w \cdot \left(\begin{bmatrix} k_x & 0 \\ 0 & k_y \end{bmatrix}\nabla v\right)d\Omega - \int_{\Omega} \nabla w \cdot \left(\begin{bmatrix} k_x & 0 \\ 0 & k_y \end{bmatrix}\nabla g\right)d\Omega = 0 \tag{22}$$

To convert the weak form of Eq. (22) to matrix form, the functions of w, v and g are approximated by NURBS basis functions and $\overline{k}$ are given by

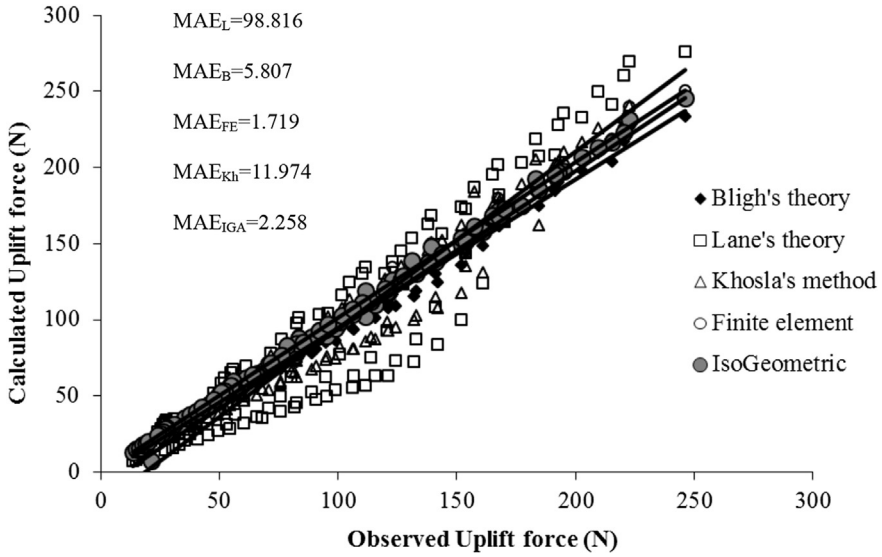

Fig. 8. Evaluation of different methods to estimate total uplift force.

$$w = R_I\overline{w},\ v = R_I\overline{v},\ g = R_D\overline{g}\ ,\ \overline{k} = \begin{bmatrix} k_x & 0 \\ 0 & k_y \end{bmatrix} \tag{23}$$

Where R_I and R_D are the inner and essential boundary NURBS basis functions, respectively. Thus, the matrix form of equations can be obtained as,

$$K\overline{v} = F_N + F_D \tag{24}$$

Where

$$K = \int_\Omega \nabla R_I^T \cdot \left(\overline{k}\nabla R_I\right) d\Omega,\ \ F_N = \int_\Gamma R_I^T h d\Gamma,$$
$$F_D = -\int_\Omega \nabla R_I^T \cdot \left(\overline{k}\,\nabla R_D\right) d\Omega\overline{g} \tag{25}$$

In Eq. (25), $\overline{g}$ can be estimated from two approaches. In first approach, the head of boundary control points is imposed by evaluating the function of boundary condition at the spatial locations of the control points. This method suffers from two essential drawbacks. When the position of boundary control points is not located on the desired boundary, it is not reasonable to enforce the given boundary heads to the corresponding boundary control variables. In the second approach, the vector of $\overline{g}$ is obtained based on interpolation of a function on the boundary. It offers a far higher rate of convergence in comparison with the first approach. Whereas in this research amount of essential boundary condition was located on control points, the first technique was utilized to apply essential boundary condition.

4.2. Data for geometry parametrisations

The IGA approach was developed for the dam foundation using dimensions and specifications of an experimental model. For all discretizations equally spaced open knot vectors are used in each direction. The polynomial degrees, knot vectors and control points for the geometry of the analytical problem were given in Table 1. Fig. 5 shows domain of the dam foundation for both without and with cutoff wall. Furthermore, the model definition where there is an vertical impermeable partition to flow beneath of the dam was illustrated in Fig. 5(b). The boundary condition on the upstream side of the dam is a total head value equal to the elevation of the water in the reservoir. On the downstream side, the boundary

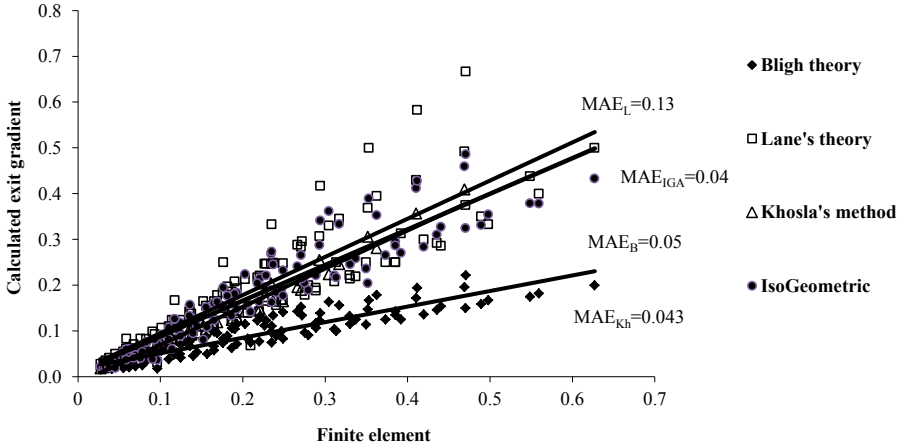

Fig. 9. Evaluation of different methods to estimate exit gradient.

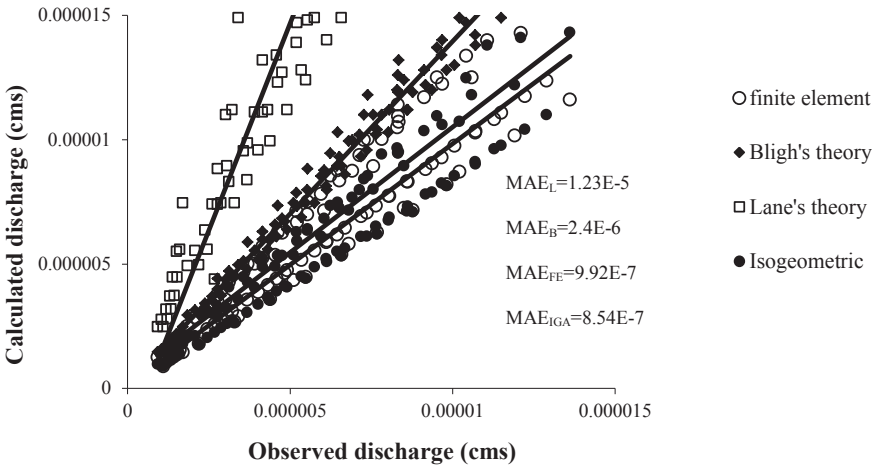

Fig. 10. Evaluation of different methods to estimate seepage discharge.

condition is set to a head value that can be equal to zero or other amount which indicates downstream any value for tail water elevation.

A view of the mesh within the dam foundation in two cases with and without cutoff wall was shown in Fig. 6.

5. Results and discussion

5.1. The realibility and accuracy of IGA and FE methods

In order to obtain the realibility and accuracy of the IGA and FE methods, the sequence of meshes were used for modeling of dam foundation. The meshes consist of coarse, medium and fine meshes by 6, 200 and 800 elements for IGA and 69, 266 and 1064 elements for FE methods, respectively. Also, we defined the relative error as the error normalized by the corresponding value of the numerical solution for seepage discharge and uplift force parameters. Convergence results for the relative error are shown in Fig. 7.

5.2. Experimental versus theorical and numerical results

In Figs. 8–10 the results of uplift force, exit gradient and seepage discharge obtained from experimental tests versus the results obtained from Bligh, Lane, Khosla et al., IGA and FE methods are indicated. As shown in Fig. 8, the accuracy of IGA and FE methods to estimate uplift force are nearly equal, while the accuracy of Lane's method is the least amount.

Since it is impossible to obtain experimentally the amount of exit gradient, the FE method employed in Geostudio2007 software was used to determine exit gradient. In Fig. 9, the results for exit gradient obtained from FE method versus the results obtained from Bligh, Khosla et al., Lane and IGA methods are indicated. As shown in Fig. 9, the accuracy of IGA method is greater of other methods and the results of Khosla's method is near to IGA method.

Also, Fig. 10 shows that the accuracy of IGA method on estimating of seepage discharge is excellent.

To make a quantitative evaluation of the accuracy of the proposed methods, two statistical error parameters were used: mean absolute error (MAE) and correlation coefficient (RSQ) defined as

$$\mathrm{RSQ} = 1 - \frac{\sum_{i=1}^{n} (x_i - \hat{x})^2}{\sum_{i=1}^{n} (x_i - \bar{x})^2} \tag{26}$$

$$\mathrm{MAE} = \frac{1}{n} \sum_{i=1}^{n} |x_i - \hat{x}_i| \tag{27}$$

Where x_i is the observed data, $\hat{x}_i$ is the calculated data and $\bar{x}_i$ is the average of observed data. The amounts of MSE and RSQ parameters for different parameters were represented in Table 2.

5.3. Estimating exit gradient using Khosla et al. Equation, FEM and IGA

To obtain results of Eq. (4) with more accurate prediction of the exit gradient, in the no cutoff wall case at downstream, the exit gradient is assumed to be infinite. Therefore a cutoff wall at the downstream end with various heights of 5, 10, 15, 20 and 30 cm under the upstream fixed head of 2.5, 5, 7.5, 10, 12.5, 15, 17.5 and 20 cm are considered and compared the obtained IGA results with the results achieved from Khosla method. The performance of results were indicated in Fig. 11. From the Fig. 11, it can be seen that predicting the exit gradient by Khosla method is nearly 27% and 33% lower than those estimated by the IGA and FE method, respectively. Considering Fig. 10, a new equation is introduced in the form of Eq. (4) to estimate exit gradient using IGA as

$$\frac{i_{exit}\, d}{H} = \frac{1}{\pi\sqrt{Y}} = 0.5586\alpha^{-0.528} \tag{28}$$

Table 2
Statistical error parameters given by different models based on experimental data sets.

		MAE	RSQ
Hydraulic gradient	Bligh	0.05	0.81
	Lane	0.13	0.756
	Khosla	0.043	0.978
	IsoGeometric	0.046	0.966
Seepage discharge	Bligh	2.4E-6	0.985
	Lane	1.23E-5	0.854
	Finite element	9.92E-7	0.992
	IsoGeometric	8.54E-7	0.998
Uplift force	Bligh	5.807	0.962
	Lane	98.816	0.849
	Finite element	1.719	0.997
	Khosla	11.974	0.942
	IsoGeometric	2.258	0.983

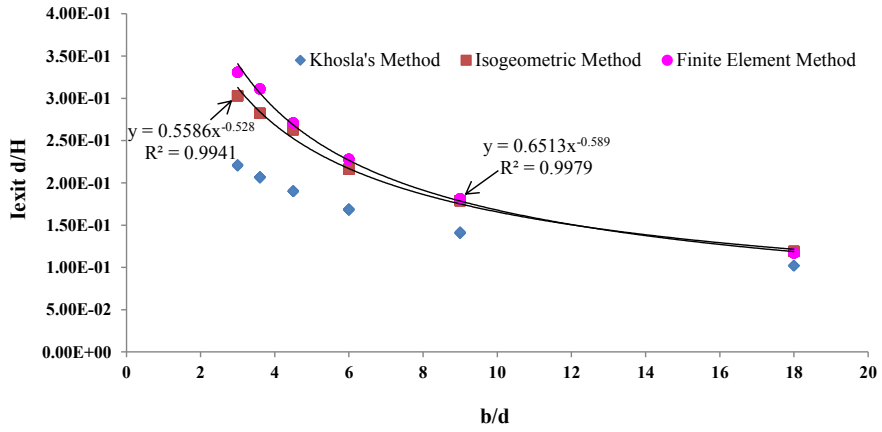

Fig. 11. Estimated exit gradient using the Khosla et al., IGA and FE Methods.

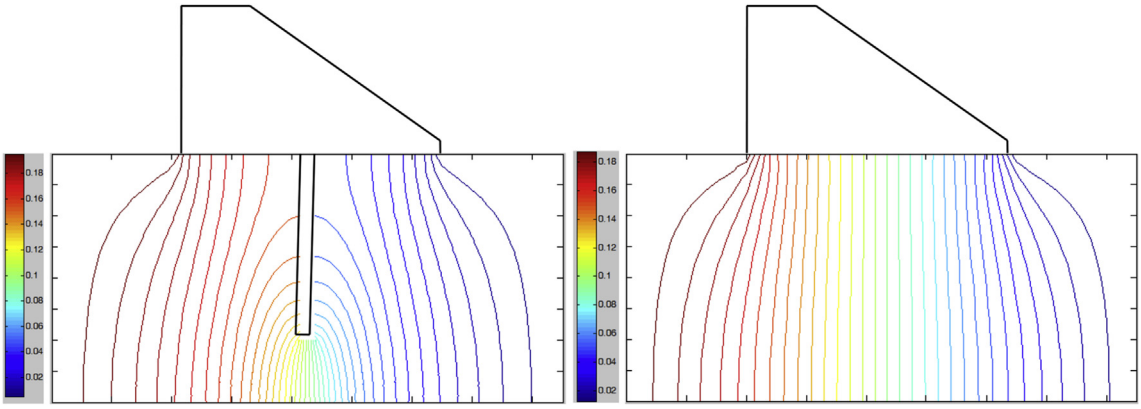

Fig. 12. Graphical results of computed heads of 20 cm at upstream and 0 at downstream for fine mesh.

$$\rightarrow Y \cong 0.3247\alpha^{1.056} \tag{29}$$

The Eq. (28) refers to the exit gradient predicted by the Eq. (4). Also, the Eq. (29) expresses the simple form of the Eq. (28).

5.4. The graphical results of computed head from IGA model

The graphical results of the head are yielded by the IGA model for both with and without cutoff wall is shown in Fig. 12. As shown in Fig. 12, the efficacy of the cutoff wall in the reduction of pressure head is indicated.

6. Conclusion

In this study, uplift pressure, seepage discharge and exit gradient were calculated using the IGA approach. The IGA model was validated using the available experimental data. For comparison conveniently, the experimental data were used to preserve the information on the relative magnitude of the different empirical and theoretical prediction such as Khosla et al., Lane and Bligh methods.

Performances of empirical, theoretical and numerical methods indicated that the IGA and FE method produced the best estimation of seepage effects. But due to size and numbers of the elements expressed in IGA compared with the FE method can be noted that the obtained results of IGA are a conceptual relationship in speed and accuracy ratio of FE method. Beside, the maximum and the minimum amount of uplift forces for the corresponding cutoff wall were characterized at the downstream and upstream of dam, respectively.

In summary, the proposed IGA method was established as a useful tool for the analysis of a wide variety of seepage problems in terms of seepage discharge, exit gradient and distribution of uplift pressure under the foundation of hydraulic structures.

Acknowledgement

The authors express their sincere thanks to Dr Tokaldani Associate professor and Mr Shayan Ph.D. student the Department of Irrigation and reclamation engineering, University of Tehran whose resources are used for this research work.

References

[1] W.G. Bligh, Dams, barrages and weirs on porous foundations, Eng. News 64 (Dec 1910) 708.
[2] S. Leliavsky, Design of Dams for Percolation and Erosion, Chapman and Hall, London, UK, 1965.
[3] E. Amiri Tokaldany, H. Khalili Shayan, Uplift force, seepage, and exit gradient under diversion dams, Proc. ICE Water Manage. 166 (8) (2012) 452–462.
[4] A.N. Khosla, N.K. Bose, E.T. McKenzie, Design of Weirs on Pervious Foundations, 1936. Publication No 12 of the central Board of Irrigation, Simla, India.
[5] J. Abedi Koupaei, Investigation of the effective elements on uplift pressure upon diversion dams by using finite difference (MSc thesis), University of Tarbiat Modarres, Tehran, Iran, 1991.
[6] J.C. Ward, Turbulent flow in porous media, J. Hydraul. Eng. ASCE 92 (4) (1964) 1–12.

[7] D. Stephenson, Rockfill in Hydraulic Engineering, Elsevier Scientific, New York, 1979, p. 230.
[8] N.M. Herrera, G.K. Felton, Hydraulics of flow through a rockfill dam using sediment-free water, Trans. ASAE 34 (3) (1991) 871–875.
[9] S.M. Hosseini, Development of an unsteady nonlinear model for flow through coarse porous media, School of Eng., (PhD. thesis), The University of Guelph, Guelph, Canada, 1997, p. 562.
[10] B. Li, V.K. Garga, M.H. Davies, Relationship for non-Darcy flow in rockfill, J. Hydraul. Eng. ASCE 124 (2) (1998) 206–212.
[11] R. Al-Raoush, K. Thompson, C.S. Wilson, Comparison of network generation techniques for unconsolidated porous media, Soil Sci. Soc. Am. J. 67 (2003) 1678–1700.
[12] R.C. Acharya, S.E. Zee, A. Leijnse, Porosity-permeability properties generated with a new 2-parameter 3D hydraulic pore-network model for consolidated and unconsolidated porous media, Adv. Water Resour. 27 (2004) 707–723.
[13] T.J.R. Hughes, J.A.Y. Cottrell, Y. Bazilevs, Isogeometric analysis: CAD, finite elements, NURBS, exact geometry and mesh refinement, Comput. Methods Appl. Mech. Eng. 194 (2005) 4135–4195.
[14] Y. Bazilevs, L.D. Veiga, J. Cottrell, T.J. R Hughes, G. Sangalli, Isogeometric analysis: approximation, stability and error estimates for h-refined meshes, Math. Models Methods Appl. Sci. 16 (2006) 1031–1090.
[15] Y. Bazilevs, T.J.R. Hughes, NURBS-based isogeometric analysis for the computation of flows about rotating components, Comput. Mech 43 (2008) 143–150.
[16] I. Akkerman, Y. Bazilevs, V. Calo, T. Hughes, S. Hulshoff, The role of continuity in residual-based variational multiscale modeling of turbulence, Comput. Mech. 41 (2010) 371–378.
[17] J.A. Cottrell, A. Reali, Y. Bazilevs, T.J.R. Hughes, Isogeometric analysis of structural vibrations, Comput. Methods Appl. Mech. Eng. 195 (2006) 5257–5296.
[18] Y. Bazilevs, V.M. Calo, T.J.R. Hughes, Y. Zhang, Isogeometric fluid–structure interaction: theory, algorithms and computations, Comput. Mech. 43 (2008) 3–37.
[19] D.J. Benson, Y. Bazilevs, M.C. Hsu, T.J.R. Hughes, Isogeometric shell analysis: the Reissner–Mindlin shell, Comput. Methods Appl. Mech. Eng. 199 (2010) 276–289.
[20] T.J.R. Hughes, A. Reali, G. Sangalli, Duality and unified analysis of discrete approximations in structural dynamics and wave propagation comparison of p-method finite elements with k-method NURBS, Comput. Methods Appl. Mech. Eng. 197 (2008) 4104–4124.
[21] J.A.Y. Cottrell, T.J.R. Hughes, Y. Bazilevs, Isogeometric Analysis Toward Integration of CAD and FEA, A John Wiley and Sons, Ltd, Publication, 2009, p. 79.